

CKM UNITARITY ANGLES $\alpha(\phi_2)$ AND $\gamma(\phi_3)$

A. JAWAHERY

Department of Physics, University of Maryland, College Park, MD 20742, U.S.A

E-mail: jawahery@physics.umd.edu

I report on the experimental studies of the CKM unitarity angles $\alpha(\phi_2)$ and $\gamma(\phi_3)$ with emphasis on recent measurements by the Belle and BaBar experiments at the B -factory accelerators.

1. Introduction

In the Standard Model, the origin of CP-violation lies in the charged weak interaction sector, which involves transitions amongst quarks of different flavor and charge through the emission of a virtual W . The coupling strengths of these transitions for the 3 generations of quarks form a 3×3 matrix first introduced by M. Kobayashi and T. Maskawa¹ and known as the (CKM) matrix. The CKM matrix is a unitary matrix parameterized by 3 real angles and one complex phase. This single complex phase of the CKM matrix is the source of CP-violation in the Standard Model (SM). A popular parametrization of the CKM matrix, by L. Wolfenstein,² is given below, where the 4 parameters are A , λ , ρ and η :

$$V_{\text{CKM}} = \begin{pmatrix} 1 - \frac{\lambda^2}{2} & \lambda & A\lambda^3(\rho - i\eta) \\ -\lambda & 1 - \frac{\lambda^2}{2} & A\lambda^2 \\ A\lambda^3(1 - \rho - i\eta) & -A\lambda^2 & 1 \end{pmatrix}.$$

The parameter η controls the CP-violating effects in this framework. The values of the CKM parameters are not specified by the SM and must be determined from experimental measurements. A review of the measurements of the magnitudes of the CKM matrix elements is given by K. Schubert at this conference, reporting values of $\lambda = 0.2235 \pm 0.0033$ and $A\lambda^2 = 0.0415 \pm 0.0011$. Information on the parameters ρ and η can be obtained from a global fit (hereafter referred to as the “CKM fit”) to several measured quantities in the K and B meson systems, including $|V_{ub}|$, $B^0 \leftrightarrow \bar{B}^0$ oscillation frequencies Δm_d and Δm_s , and CP-violation observables in the neutral kaon system (ϵ_K), whose values in the framework of the SM depend on these parameters (Fig. 1).³ For the (ρ, η) values in the small overlap region in Fig. 1, the SM can accommodate all of the above observables, of which the CPV effect in the kaon system imposes the requirement of a non-zero value for η . An interesting and important conse-

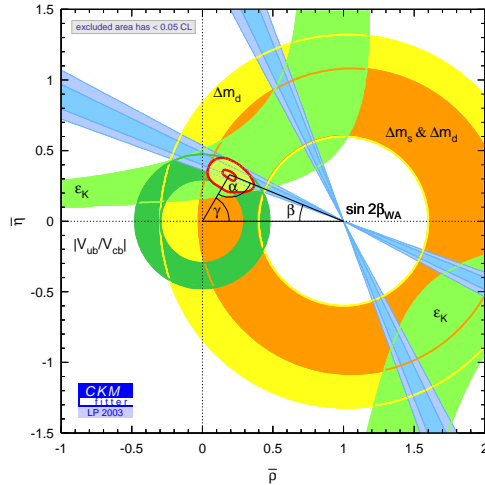


Figure 1. The “CKM fit” to data from the CKMfitter group (<http://ckmfitter.in2p3.fr/>). See the text for more details.

quence of a non-zero complex parameter in the CKM matrix is CP-violation in other particle systems, notably the decays of charged and neutral B mesons. The primary mission of the B -factory experiments is to search for the breaking of the CP-symmetry in B meson decays and examine the consistency of the measurements with the expected values within the CKM mechanism. A deviation from the SM could be an indication of New Physics effects.

1.1. Definition of the CKM Unitarity Angles and CPV Observables in B Decays

The unitarity of the CKM matrix imposes 9 complex relations amongst the matrix elements, the most famous of which is the so-called CKM unitarity triangle, shown below and pictured in Fig. 2:

$$V_{ub}^* V_{ud} + V_{cb}^* V_{cd} + V_{tb}^* V_{td} = 0.$$

The sides of this triangle are determined (or constrained) by the values of the CKM matrix elements.

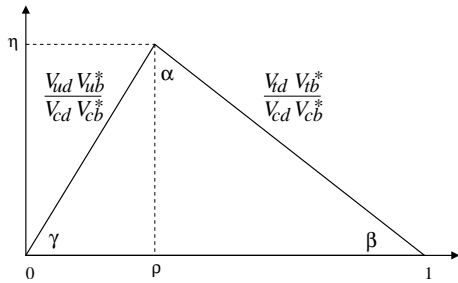


Figure 2. The CKM unitarity triangle.

The three angles:

$$\alpha(=\phi_2) = \arg \left[-\frac{V_{td}V_{tb}^*}{V_{ud}V_{ub}^*} \right],$$

$$\beta(=\phi_1) = \arg \left[-\frac{V_{cd}V_{cb}^*}{V_{td}V_{tb}^*} \right], \text{ and}$$

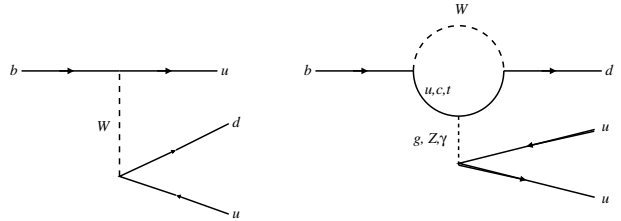
$$\gamma(=\phi_3) = \arg \left[-\frac{V_{ud}V_{ub}^*}{V_{cd}V_{cb}^*} \right]$$

can be extracted from the measurements of CP-violating effects in B meson decays. The experimental goal is to measure the three angles, which along with the knowledge of the sides of the triangle will overconstrain the model and reveal possible deviations from the SM.

The measurements of $\sin 2\beta$, the CP-violating asymmetry in B^0 decays to charmonium final states ($b \rightarrow c\bar{c}s$), by the BaBar and Belle collaborations established the breaking of CP-symmetry in B decays.⁴ The experimental status of $\sin 2\beta$ measurements are reviewed at this conference by T. Browder. The knowledge of $\sin 2\beta$ leads to four possible solutions in the (ρ, η) plane as shown in Fig. 1, one of which coincides with the allowed region from the ‘‘CKM fit’’. The fit also yields the allowed ranges $77^\circ < \alpha(\phi_2) < 122^\circ$, $37^\circ < \gamma(\phi_3) < 80^\circ$ at 95% CL, which set a reference point for comparison with direct measurements.

1.2. Experimental Strategies for Extracting Angles α and γ

Since the angles α and γ essentially measure the phase of the CKM element V_{ub} relative to other matrix elements, any experimental strategy must involve the tiny component of B decays which occur through the $b \rightarrow u$ transition. The obvious candidate channels for experimental studies are the so-called ‘‘charmless’’ B decays, such as $B \rightarrow \pi\pi$, $B \rightarrow \rho\pi$ and $B \rightarrow \rho\rho$ which can arise from the tree level transition $b \rightarrow u(\bar{u}d)$, carrying the CKM element V_{ub} (Fig. 3 (left)). However, a complication to this ap-

Figure 3. The tree (left) and penguin (right) diagrams contributing to ‘‘charmless’’ B decay ($B \rightarrow \pi\pi$, $B \rightarrow \rho\rho, \dots$).

proach arises from the presence of loop level (penguin) processes (Fig. 3 (right)), involving different CKM matrix elements, which can also lead to the same final states. The interference of the two diagrams then obscures the connection between the CP observables and the angles α and γ , thus the experimental program must also include a ‘‘tree and penguin disentanglement’’ strategy.

Complementary methods, free of penguin effects, for the determination of γ have also been explored experimentally and will be discussed in Secs. 6 and 7. These approaches involve CPV measurements in decay modes which can occur through both the CKM suppressed $b \rightarrow uW^-$ transition and the dominant $b \rightarrow cW^-$ diagram, with the interference effects providing the sensitivity to CPV phases.

1.2.1. CPV observables in ‘‘charmless’’ B decays

Two sets of experimental observables are explored for CP-violation studies in charmless B decays. For a given final state f with CP conjugate \bar{f} , the mean branching ratio and the time integrated direct CP-asymmetry, defined as:

$$A_{CP}^{direct} = \frac{\Gamma(\bar{B} \rightarrow \bar{f}) - \Gamma(B \rightarrow f)}{\Gamma(\bar{B} \rightarrow \bar{f}) + \Gamma(B \rightarrow f)}$$

acquire sensitivity to the angle γ as a result of the interference between the tree and penguin diagrams. This can easily be seen in the dependence of the decay amplitudes for the $B \rightarrow f$ and $\bar{B} \rightarrow \bar{f}$:

$$A = -(|T|e^{i\gamma} + |P|e^{i\delta}), \text{ and}$$

$$\bar{A} = -(|T|e^{-i\gamma} + |P|e^{i\delta});$$

resulting in:

$$BR \propto 1 + 2\left|\frac{P}{T}\right| \cos\delta \cos\gamma + \left|\frac{P}{T}\right|^2$$

$$A_{cp} = -2\left|\frac{P}{T}\right| \sin\delta \sin\gamma$$

where T and P are the amplitudes of the tree and penguin diagrams, respectively, and δ is the relative strong phase of the two amplitudes.

Another set of observables are the CP-violating quantities extracted from the time evolution of neutral B decays to final states that are common to B^0 and \bar{B}^0 mesons. Time dependent CP-asymmetry results from the interference of two possible paths for reaching the same final state: $B^0 \rightarrow f$ and $B^0 \leftrightarrow \bar{B}^0 \rightarrow f$. All CP-violation information is encoded in the parameter:

$$\lambda_f = \eta_{fCP} \frac{p}{q} \frac{\bar{A}}{A},$$

where $A = |\langle f|T|B^0\rangle|$, $\bar{A} = |\langle f|T|\bar{B}^0\rangle|$, η_{fCP} is the CP-eigenvalue of the final state and $\frac{p}{q}$ is a measure of CPV in mixing. Observation of either $\arg(\lambda_f) \neq 0$ or $|\lambda_f| \neq 1$ would indicate the presence of CPV in the final state f . Time dependent CP-asymmetry follows:

$$A_{cp}(\Delta t) = S_f \sin(\Delta m_d \Delta t) - C_f \cos(\Delta m_d \Delta t)$$

where the observables $S_f = \frac{2\Im(\lambda_f)}{1+|\lambda_f|^2}$ and $C_f = \frac{1-|\lambda_f|^2}{1+|\lambda_f|^2}$ measure the so-called indirect CP violation resulting from interference of decay and mixing, and direct CP violation in the decay ($|A| \neq |\bar{A}|$), respectively. In the simplest case where the decay is dominated by a single tree diagram, $\lambda_f = \eta \frac{V_{tb}^* V_{td} V_{ub} V_{ud}^*}{V_{tb} V_{td}^* V_{ub}^* V_{ud}} = e^{i2\alpha}$, $C_f = 0$, thus $S_f = \sin 2\alpha$. However, in general, with the penguin contribution present, one has:

$$\lambda_f = e^{2i\alpha} \frac{1 + |\frac{P}{T}| e^{i\delta} e^{i\gamma}}{1 + |\frac{P}{T}| e^{i\delta} e^{-i\gamma}},$$

resulting in $C_f \neq 1$ and $S_f = \sqrt{1 - C_f^2} \sin 2\alpha_{eff}$ (see the References^{14,16} for more details.). The net effect of the penguin presence is to introduce the possibility of direct CP-violation ($C_f \neq 1$) and a possible shift of $\Delta\alpha = \alpha_{eff} - \alpha$, the magnitude of which would depend on the ratio $|P/T|$ and the strong phase δ .

The presence of “non-tree” level diagrams in charmless decays is inferred from the observed pattern of the branching ratios in these modes, as seen in the compilation of the data for the 2-body charmless decays by the Heavy Flavor Averaging Group.⁵ At the tree level the expected rate for the CKM suppressed decay $B^0 \rightarrow K^- \pi^+$ would be about 5% of the rate for $B^0 \rightarrow \pi^+ \pi^-$. However, the pattern of the data does not follow this expectation; the measurements (initially by CLEO) give $B(B^0 \rightarrow K^- \pi^+) = (18.2 \pm 0.8) \times 10^{-6}$ and $B(B^0 \rightarrow \pi^- \pi^+) = (4.6 \pm 0.4) \times 10^{-6}$. This enhancement of

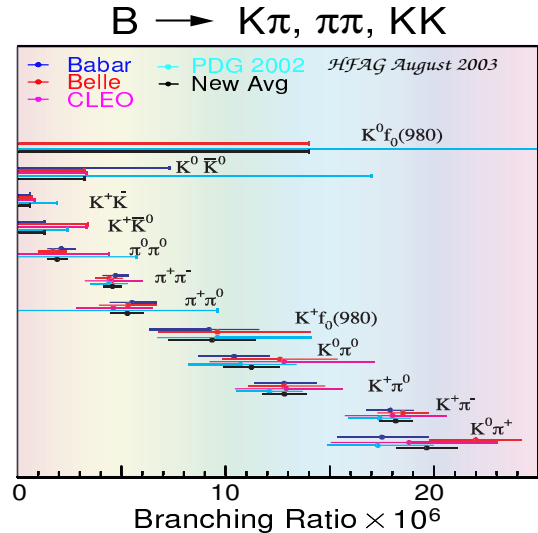


Figure 4. Summary of branching ratios for charmless 2-body B decays by the Heavy Flavor Averaging Group.

the $K\pi$ mode, also observed in the rest of the family of $K\pi$ and $\pi\pi$ modes, is an indication of the presence of another process contributing at a significant level to these decays. The main candidates within the Standard Model are the radiative loop diagrams (penguins), dominated by the QCD penguins. The experimental investigation of charmless decays aiming at the determination of the angles α and γ from these modes is performed with the reality of the penguin contribution in mind. It is clear that no single measurement in these channels is likely to lead to the determination of α and γ . The answer is likely to arise from exploiting the connections (via isospin symmetry, SU(3) of flavor) amongst the rates and CP-asymmetries of many modes, along with the use of factorization and perhaps other more predictive theories such as QCD factorization⁶ or perturbative QCD⁷ (when independently verified). This requires a comprehensive experimental and theoretical analysis of all pieces of the “charmless” puzzle, which forms the basis of the knowledge of α and γ .

2. Experimental Arrangement at the B -factories

The B -factory experiments, BaBar at the PEP-II machine at SLAC and Belle at the KEKB machine in the KEK laboratory in Japan, have been designed and optimized to study time-dependent CP-violation

in B decays at the $\Upsilon(4S)$. The detailed description of the machines and the detectors can be found elsewhere. Here I will briefly summarize the main features of the experimental arrangement, in particular the aspects pertaining to the study of charmless B decays. The B -factories are asymmetric electron-positron colliders operating at a center-of-mass energy near the $\Upsilon(4S)$ (10.58 GeV) resonance. The $\Upsilon(4S)$ is just above the threshold for open Bottom (B) production and decays exclusively to a B^+B^- or $B^0\bar{B}^0$ pair, with nearly equal proportion. Close to the threshold, B 's are produced nearly at rest in the center-of-mass frame of the $\Upsilon(4S)$. The $\Upsilon(4S)$ resonance, which produces a cross section peak of about 1 nb^{-1} on a continuum background of about 3 times larger, has been mined in the past 20 years by the CLEO experiment at the CESR machine at Cornell and the ARGUS experiment at the DORIS-II machine in DESY, for exploring properties of the B mesons. The new machines (PEP-II and KEKB) have earned the title of “Factory” because of their high luminosities, which is required for producing large number of B 's for CPV studies. The other new feature is their asymmetric laboratory beam energies: 9 GeV e^- on 3.1 GeV e^+ for PEP-II and 8 GeV e^- on 3.5 GeV e^+ for KEKB, resulting in a relativistic boost to the B mesons, which allows for mapping the time-evolution of “tagged” neutral B decays. “Tagged” here refers to the identification of the initial flavor (b or \bar{b}) of the B meson at the $\Delta t = 0$. Since the B^0 meson undergoes flavor oscillation before decaying, information on its initial flavor is extracted from the flavor of the other B meson in the event, taking advantage of the quantum entangled nature of the “ $B^0\bar{B}^0$ ” system in an $L=1$, $CP=-1$ state, which by spin statistics forbids the pair to transform into a B^0B^0 or a $\bar{B}^0\bar{B}^0$ state, hence correlating the flavor of the two B mesons until one of them decays. The particle content and the kinematical properties of the decay products of the B meson reveal its (B or \bar{B}) flavor. The experiments perform decay time measurements using precision silicon vertex tracking, and particle identification using a variety of techniques, including electromagnetic calorimetry, measurement of dE/dx in the tracking system and Čerenkov detectors. Charmless 2-body B decays pose a particularly difficult experimental problem for hadron identification, as π/K discrimination is crucial to separating the overlap-

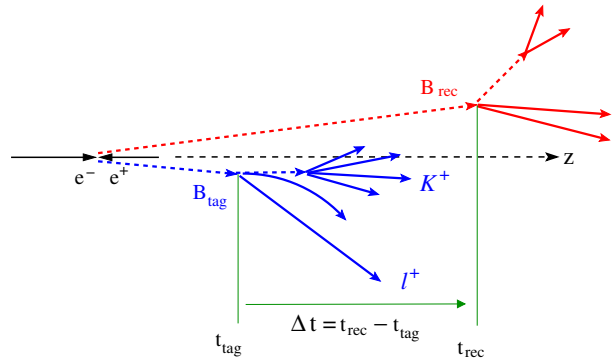


Figure 5. A cartoon of a $B\bar{B}$ event at an asymmetric B -factory. See the text for more detail.

ping $B \rightarrow \pi\pi$ and $B \rightarrow K\pi$ modes, whose decay products populate the momentum range of 1-4 GeV in the laboratory frame.

A cartoon of a $B\bar{B}$ event produced in an asymmetric B -factory is shown in Fig. 5, depicting the decay products of a pair of B mesons boosted along the beam direction (the z -axis). In such a scenario one B meson decays into a rare CP-eigenstate such as $B \rightarrow \pi^+\pi^-$ (B_{cp}) and the other B in a generic “flavor revealing” mode (B_{tag}). For a fully reconstructed B meson, two kinematical quantities can be constructed from measurements of its decay products and the knowledge of the colliding beam energies, all calculated in the center-of-mass frame: beam energy constrained mass defined as $M_{ES} = \sqrt{E_{\text{beam}}^2 - P_B^{*2}}$ and the energy difference $\Delta E = E_{\text{beam}} - E_B^*$, where E_{beam}^* is half of the total center-of-mass energy and P_B^* and E_B^* are the reconstructed momentum and energy of the B meson candidate. The experimental resolution of M_{ES} is dominated by the knowledge of the beam energy and is typically around 2 to 3 MeV. The resolution in ΔE is dominated by the E_B^* resolution, thus its value is mode dependent with a range of 15-30 MeV, for modes with only charged tracks in the final state.

Quantities central to a CP analysis of B meson decays are decay vertex separation along the beam axis $\Delta Z = Z_{\text{tag}} - Z_{cp}$ and the flavor tagging information from the decay products of the other B in the event. The decay time difference is extracted from the relation $\Delta t \simeq \Delta Z / \gamma\beta$, with a typical resolution of around $180 \mu\text{m}$, dominated by the vertex measurement on the tagging side. Flavor tagging is achieved with an effective efficiency $\epsilon(1-2w)^2 \simeq 30\%$, where ϵ

and w are the tagging efficiency and the mis-tagging probability, respectively.

Charmless B decays of interest to CP analysis require additional experimental attention. Typically, the relevant branching ratios are of the order of 10^{-5} or less and their kinematical features are readily mimicked by the copious continuum $e^+e^- \rightarrow q\bar{q}$ events. Furthermore, the modes of similar topology, such as $B \rightarrow \pi\pi$, $B \rightarrow K\pi$ and $B \rightarrow KK$ have considerable overlap in the ΔE distribution. A number of experimental handles exploiting the differences in event shape properties of $B\bar{B}$ and continuum $q\bar{q}$ events have been developed to suppress the background effects. The powerful hadron identification capabilities of the detectors are the key to separating modes of similar topologies.

3. CP-violation Studies with 2-body Charmless B Decays

The B -factory experiments have performed comprehensive studies of the branching ratios and CP-asymmetries in 2-body charmless decays $B \rightarrow \pi\pi$ and $B \rightarrow K\pi$, improving significantly over the previous measurements from the CLEO experiment. Below, I will discuss the latest measurements of the time-dependent CP-asymmetries in $B \rightarrow \pi^+\pi^-$ and results on the first observation of the decay $B \rightarrow \pi^0\pi^0$, followed by a summary of the measurements of 2-body charmless decays and comments on the implication of these results for the angles α and γ .

3.1. CP Analysis of the Decay $B \rightarrow \pi^+\pi^-$

Both BaBar⁸ and Belle⁹ have performed and published CPV analyses of the decay $B \rightarrow \pi^+\pi^-$. The published results are based on data samples of 81 fb^{-1} for BaBar and 78 fb^{-1} for Belle, collected up to the summer conferences in 2002. The BaBar collaboration has updated their measurements for this conference by including their Run 3 data and the reprocessed Run 1 and Run 2 data samples, totaling 113 fb^{-1} at the $\Upsilon(4S)$ peak. The measurements from the Belle collaboration were not updated for this conference.

For their 2002 results, each experiment observes about 200 events in this channel, with comparable signal-to-noise ratio of $S/B \simeq 1$. The quality of the signals and the relative contributions of the

backgrounds can be seen in the ΔE distributions in Figs. 6 (Belle) and 7 (BaBar).

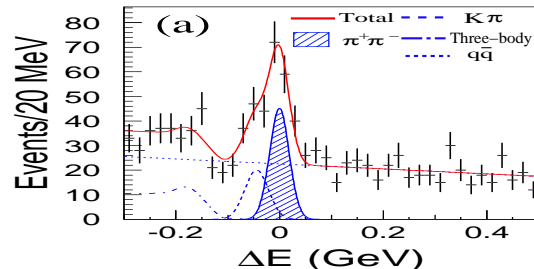


Figure 6. ΔE distribution for $B \rightarrow \pi^+\pi^-$ candidates in the Belle data (2002).

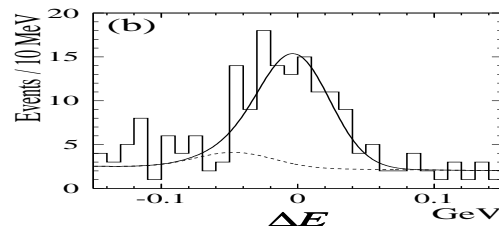


Figure 7. ΔE distribution for $B \rightarrow \pi^+\pi^-$ candidates in the BaBar data (2002).

These distributions are obtained after applying cuts on various variables developed for background suppression, including particle identification criteria. The distribution for the BaBar data is a projection plot, where the cut is applied on the signal-to-background likelihood ratio, which is constructed from the distributions of the various quantities used in the analysis. The ΔE distributions show the residual $K\pi$ component, which is present in the distribution of the signal candidates, the size of which depends on the K/π separation of the experiment. In the CP analysis, the Δt and “tagging” information are added to the kinematical and event shape quantities to perform an unbinned maximum-likelihood fit to the event sample in order to extract the values of the CP observables, $S_{\pi\pi}$ and $C_{\pi\pi}$. For details of the methods in each case, see the published papers on the subject.^{8,9} The results are summarized in Table 1, including the updated BaBar results with 113 fb^{-1} , which supersedes their previous measurement. The Δt distributions and the CP-asymmetries are shown in Fig. 8 for the BaBar measurement (2003) with their full data sample, including Run 3, and in Fig. 9

for the Belle measurement (2002). The BaBar and Belle results have a χ^2 of 6.7 for 2 degrees of freedom, which corresponds to about a 2σ separation. A simple average of the two measurements is given in Table 1. There is no significant evidence for direct CPV ($C_{\pi\pi} \neq 0$) or indirect CPV ($S_{\pi\pi} \neq 0$) in this channel. Further discussion of the implications of the results and possible constraints on the CKM unitarity angle α are presented in Sec. 4.

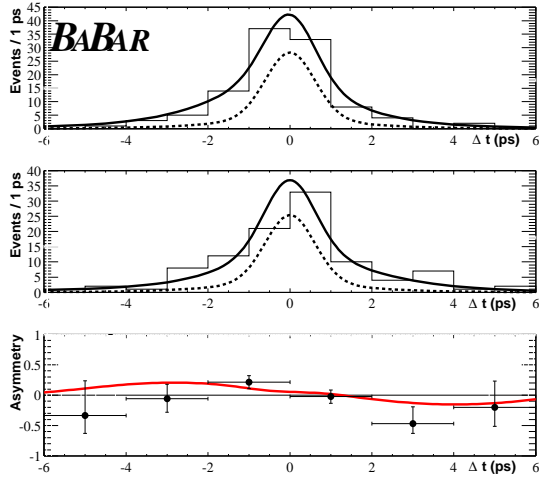


Figure 8. The Δt distributions of $B \rightarrow \pi^+\pi^-$ candidates in the BaBar data, including their Run 3 data sample. The measured time dependent asymmetries are shown in the bottom plot.

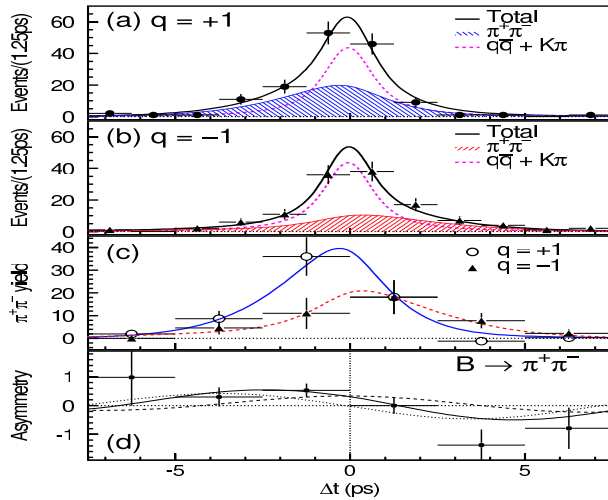


Figure 9. The Δt distributions of $B \rightarrow \pi^+\pi^-$ candidates in the Belle data. The measured time dependent CP asymmetries are shown in the bottom plot.

3.2. Observation of the Decay $B \rightarrow \pi^0\pi^0$

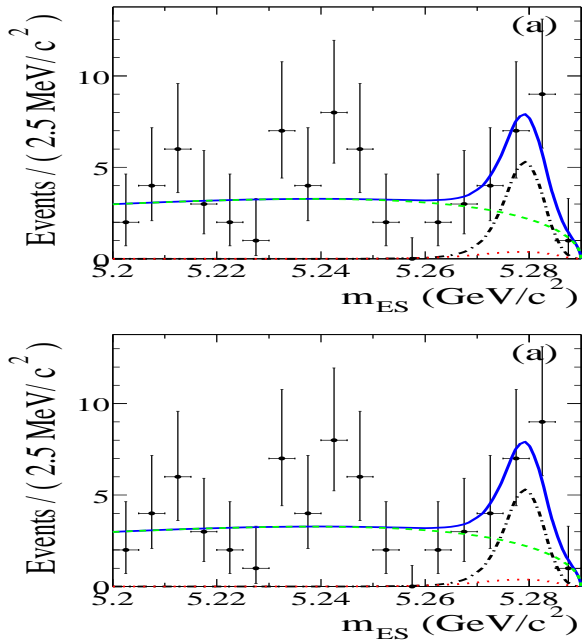
Perhaps the most pleasant new input of relevance to the angle α at this conference is the observation of the decay $B \rightarrow \pi^0\pi^0$ by the BaBar collaboration,¹⁰ supported by strong evidence from the Belle collaboration.¹¹ The decay $B \rightarrow \pi^0\pi^0$ is one of the components of the isospin analysis, which allows for disentangling the penguin and tree effects in charmless 2-body B decays. Previous results in this mode were limited to upper bounds (at 90% CL) on its branching ratio: $< 3.6 \times 10^{-6}$ for BaBar, $< 6.4 \times 10^{-6}$ for Belle and $< 4.4 \times 10^{-6}$ for CLEO.

The new BaBar result is based on their full data set of 113 fb^{-1} , which represents a 40% enhancement in statistical power of the data. Two major improvements were also introduced in the analysis. A major source of background in this analysis is the decay $B \rightarrow \rho^+\pi^0$, whose branching ratio was recently measured by the BaBar collaboration to be: $(B(B \rightarrow \rho^+\pi^0) = (11.0 \pm 1.9 \pm 1.9) \times 10^{-6})$, significantly lower than the previous upper bound from the CLEO experiment ($B(B^+ \rightarrow \rho^+\pi^0) < 43 \times 10^{-6}$ at 90% CL). This results in a lower level (and lower uncertainty) for the estimated background from this source. The second analysis improvement is the new optimization of the Fischer discriminant (F), which is a linear combination of several signal and continuum background discriminating variables and includes the output of a neural network program on “flavor tagging” analysis. The M_{ES} and (F) distributions of the $\pi^0\pi^0$ candidates are shown in Fig. 10, where a clear peak is evident at the B mass. The small estimated background from $B \rightarrow \rho^+\pi^0$ is shown in the dashed curve. The signal is, by choice of binning, distributed uniformly in the F variable (solid histogram), whereas the background $q\bar{q}$ events are represented by the rising dashed histogram. There is a clear excess of events above the expected background in the first bin, which is the most discriminating region of the distribution. From a fit to the data, the BaBar collaboration reports 46^{+14+2}_{-13-3} events in the $B \rightarrow \pi^0\pi^0$ decay. The overall significance of the effect, including the systematic uncertainties, is 4.3σ , qualifying it for an “Observation” report. They report a branching ratio of $(2.1 \pm 0.6(\text{stat}) \pm 0.3(\text{syst})) \times 10^{-6}$.

The Belle collaboration also presents strong evidence for this mode, using their full data set of 158 fb^{-1} on the $\Upsilon(4S)$ peak. The distributions of

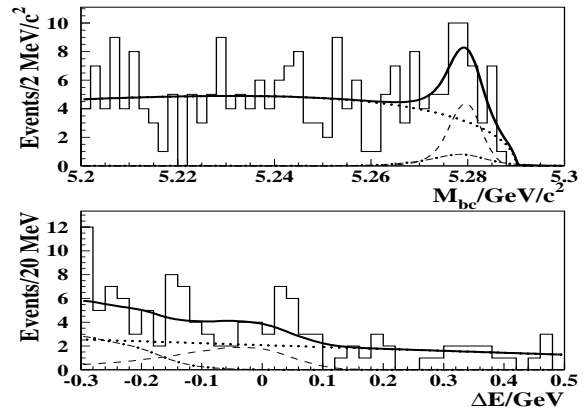
Table 1. Measurements of $S_{\pi\pi}$ and $C_{\pi\pi}$ by the BaBar and Belle experiments.

Experiment	Data sample	$S_{\pi\pi}$	$C_{\pi\pi}$
BaBar(2002)	81 fb ⁻¹	$0.02 \pm 0.34 \pm 0.05$	$-0.3 \pm 0.25 \pm 0.04$
Belle(2002)	78 fb ⁻¹	$-1.23 \pm 0.41^{+0.08}_{-0.07}$	$-0.77 \pm 0.27 \pm 0.08$
BaBar(2003)	113 fb ⁻¹	$-0.40 \pm 0.22 \pm 0.03$	$-0.19 \pm 0.19 \pm 0.05$
Average (BaBar 2003 & Belle 2002)		-0.58 ± 0.20	-0.38 ± 0.16

Figure 10. Distribution of M_{ES} and Fischer discriminant (F) for $B \rightarrow \pi^0\pi^0$ candidates in the BaBar data.

their candidate events in M_{ES} and ΔE are shown in Fig. 11, along with the estimated background from $B \rightarrow \rho^+\pi^0$ using the new BaBar measurement of this branching ratio, and the estimated background from continuum $q\bar{q}$ events. A fit to the data yields $25.6^{+9.3}_{-8.4}$ events with a significance of 3.4σ . They report a branching ratio of $(1.7 \pm 0.6(stat) \pm 0.3(syst)) \times 10^{-6}$, consistent with the BaBar measurement.

With the observation of the decay $B \rightarrow \pi^0\pi^0$, all modes needed for the isospin analysis have now been identified, an important step in the overall program of measuring the angle α . The measurements of the branching ratios are summarized in Table 2, along with the world averages from the Heavy Flavor Averaging Group (HFAG).⁵

Figure 11. Distribution of M_{ES} and ΔE for $B \rightarrow \pi^0\pi^0$ candidates in the Belle data.

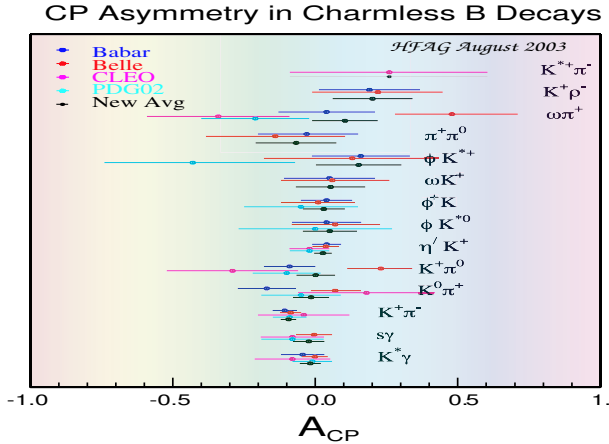
3.3. Summary of Measurements of Charmless 2-body Decays

A summary of the measured branching ratios and direct CP-asymmetries in charmless 2-body B decays has been produced by HFAG and is shown in Figs. 4 and 12. Clearly much progress has been made with the data from the B -factories. The new measurements confirm the original finding by the CLEO experiment that the penguin effects play a significant role in rare B decays. Except for the direct CP-asymmetry in the mode $B \rightarrow \pi^0\pi^0$, all other components of the isospin analysis for “the tree and penguin disentanglement” in the mode $B \rightarrow \pi\pi$ have been identified.

The improvement in the accuracy of time-integrated direct CP-asymmetries is worthy of some attention. In the mode $B^0 \rightarrow K^-\pi^+$, the experiments report: $-0.107 \pm 0.041 \pm 0.013$ (BaBar) and $-0.086 \pm 0.035 \pm 0.014$ (Belle), each at about 2.5σ from no CPV, with a world average (includ-

Table 2. Summary of the measurements of the branching ratios ($\times 10^{-6}$) of $B \rightarrow \pi\pi$ decays.

Mode	CLEO	Belle	BaBar	Average
$\pi^+\pi^-$	$4.5^{+1.4-0.5}_{-1.2-0.4}$	$4.4 \pm 0.6 \pm 0.3$	$4.7 \pm 0.6 \pm 0.2$	4.6 ± 0.4
$\pi^+\pi^0$	$4.6^{+1.8+0.7}_{-1.6-0.6}$	$5.3 \pm 1.3 \pm 0.5$	$5.5^{+1.0}_{-0.9} \pm 0.6$	5.2 ± 0.8
$\pi^0\pi^0$	< 4.4	$1.7 \pm 0.6 \pm 0.3$	$2.1 \pm 0.6 \pm 0.3$	1.97 ± 0.47

Figure 12. Summary of direct CP-asymmetries for charmless 2-body B decays by the Heavy Flavor Averaging Group (HFAG).

ing the CLEO measurement $-0.04 \pm 0.16 \pm 0.02$) of -0.09 ± 0.03 . It is also interesting that at this point there is no evidence for “large” direct CP-violation in any mode.

4. What Have We Learned About α and γ ?

To begin with, the consistency of the CPV measurements with the CKM picture in the Standard Model must be examined. I refer the reader for detail discussions of the topic to several recent reviews.^{16–18} As discussed in the previous sections, the SM reference points for the purpose of comparison with data are the expected ranges of the angles from the “CKM fit”: ($77^\circ < \alpha(\phi_2) < 122^\circ$, $37^\circ < \gamma(\phi_3) < 80^\circ$ at 95% CL). Following the approach of M. Gronau and J.L. Rosner,^{14,16} the CPV measurements are compared with theoretical predictions in the plane of ($S_{\pi\pi}$ and $C_{\pi\pi}$) (Fig. 13). $S_{\pi\pi}$ and $C_{\pi\pi}$ are computed according to the equations in Sec. 1.2, which

require as inputs the ratio of penguin to tree, $|P/T|$, and the relative strong phase of the two amplitudes (δ). In the Gronau and Rosner approach, the value of $|P/T|$ is estimated by employing factorization and SU(3) relations, and exploiting information on 2-body charmless B decays, such as the rates for the penguin dominated decay $B \rightarrow K^0\pi^+$, the tree dominated decay $B \rightarrow \pi^+\pi^0$ as well as the form factor from the semi-leptonic decay $B \rightarrow \pi\ell\nu$. A value of around 0.27 (± 0.03) is favored from these considerations. For the plot presented here a ballpark value of 0.3 is used. No constraints are imposed on δ , allowing it the full range of $-\pi$ to $+\pi$. Figure 13 illustrates the physical boundary imposed by the relation $S^2 + C^2 < 1.0$ (the large circle), the family of $C_{\pi\pi}$ vs $S_{\pi\pi}$ curves (the circles from right to left) for input values of $\alpha = 30(\text{deg.})$, $60(\text{deg.})$, $90(\text{deg.})$, $105(\text{deg.})$, $120(\text{deg.})$ and $140(\text{deg.})$. The circles corresponding to the two ends of the allowed range of α from the “CKM” fit: 77° and 122° are also labeled. The data points for BaBar (square), Belle (circle) and the “world average” (WA) (diamond) are also shown. Clearly, at the current level of predictive power of the theory and the experimental precision, the SM can accommodate the experimental measurement. Further progress in sharpening this comparison and its implication for the angle α would require independent constraints on the strong phase δ and improved accuracy on the knowledge of the value of $|P/T|$.

4.1. Constraints on α using $S_{\pi\pi}$ and $C_{\pi\pi}$ and Connections amongst 2-body Charmless B Decays

Gronau and London¹² proposed the use of isospin relations amongst rates and CP-asymmetries of $B \rightarrow \pi\pi$ decays for extracting the shift $\Delta\alpha = \alpha_{eff} - \alpha$, where α_{eff} is determined from $\sin 2\alpha_{eff} = \frac{S_{\pi\pi}}{\sqrt{1-C_{\pi\pi}^2}}$. The isospin analysis involves construction of sepa-

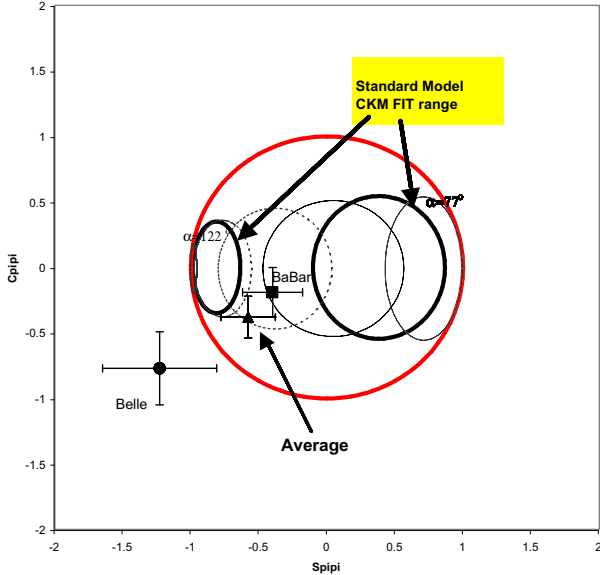


Figure 13. $C_{\pi\pi}$ vs $S_{\pi\pi}$. The physical boundary is confined to inside of the solid enveloping circle. The data points are BaBar (filled square), Belle (filled circle), and average (Diamond). See the text for further description of the graph.

rate triangles from the information on B^0 and \bar{B}^0 decays, thus requiring measurement of direct CP-asymmetries in addition to the average branching ratios into $\pi\pi$ final states (Fig. 14). The mismatch between the two triangles yields the value of $|\Delta\alpha|$, with a four-fold ambiguity. Given the current statistical power of the data, we are still some distance from achieving a useful measurement of direct asymmetry in the $\pi^0\pi^0$ mode, thus a full isospin analysis is not yet possible. Quinn and Grossman¹⁹ have shown that the knowledge of the ratio of mean branching fractions for $\bar{B}(B \rightarrow \pi^0\pi^0)$ and $\bar{B}(B \rightarrow \pi^0\pi^+)$ decays imposes an upper bound on $\Delta\alpha$ according to the following equation:

$$\sin^2\Delta\alpha < \frac{\bar{B}(B^0 \rightarrow \pi^0\pi^0)}{B(B^\pm \rightarrow \pi^\pm\pi^0)}.$$

The current data leads to $|\alpha_{eff} - \alpha| < 48^\circ$ at 90% CL, which is not a very useful constraint and given the large value of the ratio of branching ratios, no significant improvement is expected in the future. Other relations have also been developed but unfortunately with the current level of accuracy of the measurements none improves significantly over the above limit.^{20,21}

A. Hoecker, H. Lacker, M. Pivak and L. Roos¹⁸ report an analysis of the information on charmless

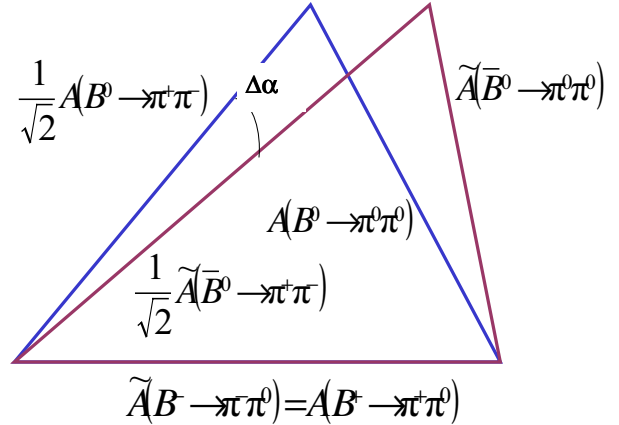


Figure 14. Isospin triangles for the $B \rightarrow \pi\pi$ system.

2-body decays, within several theoretical scenarios for connecting the various pieces of the data. These include SU(2) (isospin relations), flavor SU(3), and inputs from QCD factorization⁶ on SU(3) breaking and penguin and tree ratios and phases. They employ the tools of the “global CKMfitter” to compute confidence level for the possible values of the angle α . In Fig. 15, is plotted the confidence level vs α from a fit to the data for two scenarios: (top) SU(3) relation among various modes and an estimate of the penguin amplitude from $B \rightarrow K^0\pi^+$ and (bottom) using the QCD factorization predictions for P/T and δ . The confidence level plot from the “CKM fit” for the angle α is also shown. In both cases the “global CKM fit” has substantial overlap with fits to the data from the 2-body decays, again indicating that the SM can accommodate the data.

4.1.1. Any constraints on γ ?

The decay rates and direct CP-asymmetries in the $B \rightarrow K\pi$ channels are sensitive to the angle γ . A number of ratios of branching ratios and pseudo-asymmetries, defined below, have been proposed and examined by several authors for extracting information on γ (Rosner, Gronau, Fleischer, Neubert and Mannel).^{22–24} These are:

$$R_0 = \frac{B(B^0 \rightarrow K^+\pi^-) + B(\bar{B}^0 \rightarrow K^-\pi^+)}{B(B^0 \rightarrow K^+\pi^0) + B(\bar{B}^0 \rightarrow K^-\pi^0)} \frac{\tau(B^+)}{\tau(B^0)},$$

$$A_0 = \frac{B(B^0 \rightarrow K^+\pi^-) - B(\bar{B}^0 \rightarrow K^-\pi^+)}{B(B^0 \rightarrow K^+\pi^0) + B(\bar{B}^0 \rightarrow K^-\pi^0)} \frac{\tau(B^+)}{\tau(B^0)},$$

$$R_c = 2 \frac{B(B^+ \rightarrow K^+\pi^0) + B(\bar{B}^- \rightarrow K^-\pi^0)}{B(B^+ \rightarrow K^0\pi^+) + B(\bar{B}^- \rightarrow K^0\pi^-)},$$

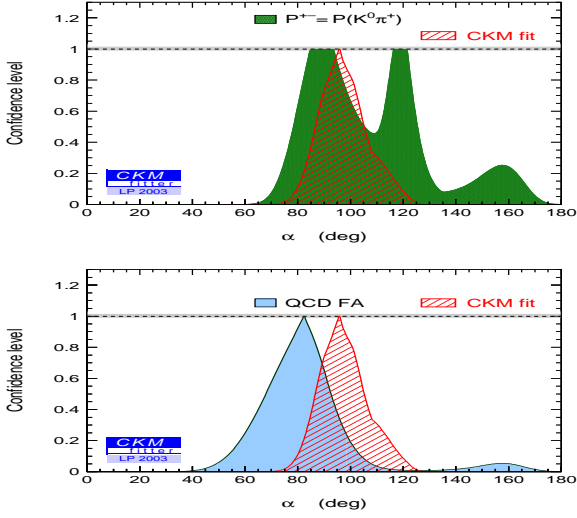


Figure 15. A global fit to the measurements of the $\pi\pi$ system. See the text for detail description of the content of the graphs.

$$A_c = 2 \frac{B(B^+ \rightarrow K^+ \pi^0) - B(\bar{B}^- \rightarrow K^- \pi^0)}{B(B^+ \rightarrow K^0 \pi^+) + B(\bar{B}^- \rightarrow K^0 \pi^-)},$$

$$R_n = \frac{1}{2} \frac{B(B^0 \rightarrow K^+ \pi^-) + B(\bar{B}^0 \rightarrow K^- \pi^+)}{B(B^0 \rightarrow K^0 \pi^+) + B(\bar{B}^0 \rightarrow K^0 \pi^0)}, \text{ and}$$

$$A_n = \frac{1}{2} \frac{B(B^0 \rightarrow K^+ \pi^-) - B(\bar{B}^0 \rightarrow K^- \pi^+)}{B(B^0 \rightarrow K^0 \pi^+) + B(\bar{B}^0 \rightarrow K^0 \pi^0)}.$$

The updated values of these ratios based on the latest world averages (from HFAG) are:

$$R_0 = 0.99 \pm 0.09 \quad A_0 = -0.09 \pm 0.03$$

$$R_c = 1.30 \pm 0.15 \quad A_c = 0.0 \pm 0.06,$$

$$R_n = 0.8 \pm 0.11 \quad A_n = -0.07 \pm 0.03.$$

Comparisons of the data with theoretical relations have been discussed by the authors mentioned above and shown that the data accommodates the range of γ from the “global CKM fit”. (For recent reviews see the References.^{16,17})

5. Other Channels for Reaching α

Extending the measurement of the angle α to higher multiplicity charmless B decay modes, such as $B \rightarrow 3\pi$ and $B \rightarrow 4\pi$, is the natural next step. The CPV studies in these channels would require the additional analysis step of isolating the CP-eigenstate components of the multiparticle system. The simplest approach would be to identify quasi-2 body decays into resonances, such as $B \rightarrow \rho\pi$, $B \rightarrow a_1\pi$, or $B \rightarrow \rho\rho$, and perform an angular analysis of the final states to isolate the CP-odd and CP-even components.

The $B \rightarrow \rho\pi$ system presents a special case for the neutral B decays: the final states $\rho^+\pi^-$ and $\rho^-\pi^+$, which can be reached by both B^0 and \bar{B}^0 , have substantial overlap in the Dalitz plot, thus their amplitudes interfere and generate additional dependence on α and the strong phases of the final states. Quinn and Snyder¹³ have shown that the interference effect can be exploited to extract the angle α even in the presence of penguins. This would involve an amplitude analysis of the 3π Dalitz distribution, which is a formidable task given the presence of large background from $q\bar{q}$ and generic $B\bar{B}$ events. Studies have shown that the sensitivity of such an analysis begins to become interesting for the B -factory data samples at around 100 fb^{-1} . Studies along these lines are currently underway in both BaBar and Belle with results expected in the next few months.

In the absence of a full amplitude analysis, BaBar has presented a CP analysis of the quasi 2-body decay $B \rightarrow \rho^\pm \pi^\mp$ ²⁵ and both BaBar and Belle have performed measurements of the branching ratios of the various modes necessary for an isospin analysis of the $\rho\pi$ system, analogous to the $\pi\pi$ system. More details on these measurements are discussed below. Both BaBar and Belle have also presented results on the decay $B \rightarrow \rho\rho$, which indicate interesting possibilities for extracting information on the angle α .

5.1. CP Studies of the Decay $B \rightarrow \rho\pi$

The system $\rho^\pm \pi^\mp$ is not a CP-eigenstate, but both final states $\rho^+\pi^-$ and $\rho^-\pi^+$ can be reached by B^0 and \bar{B}^0 , thus it is a candidate for time-dependent CP-asymmetry studies. The time evolution of a neutral B decay in this mode follows:

$$f_{B^0}(\rho^\pm h^\mp)(\Delta t) = (1 \pm A_{cp}(\rho h))e^{-|\Delta|t/\tau} (1 + [(S_{\rho h} \pm \Delta S_{\rho h})\sin(\Delta m \Delta t) - (C_{\rho h} \pm \Delta C_{\rho h})\cos(\Delta m \Delta t)]),$$

$$f_{\bar{B}^0}(\rho^\pm h^\mp)(\Delta t) = (1 \pm A_{cp}(\rho h))e^{-|\Delta|t/\tau} (1 - [(S_{\rho h} \pm \Delta S_{\rho h})\sin(\Delta m \Delta t) - (C_{\rho h} \pm \Delta C_{\rho h})\cos(\Delta m \Delta t)]),$$

Where $h = \pi$ or K . Summing over the charge of the ρ meson, results in the time-dependent asymmetry:

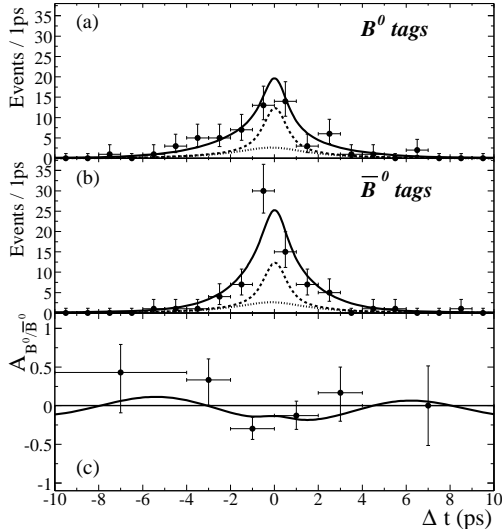
$$A_{\rho\pi}(B^0/\bar{B}^0) \simeq S_{\rho\pi}\sin(\Delta m \Delta t) - C_{\rho\pi}\cos(\Delta m \Delta t).$$

The CP-violating observables are: $S_{\rho\pi}$ for indirect

Table 3. Summary of the measurements of branching ratio ($\times 10^{-6}$) of $B \rightarrow \pi\pi$ decays.

$N(\rho\pi)$	$N(\rho K)$	$C_{\rho\pi}$	$S_{\rho\pi}$
804.2 ± 49.2	260.4 ± 31.4	$0.35 \pm 0.13 \pm 0.05$	$-0.13 \pm 0.18 \pm 0.04$
$A_{CP}(\rho\pi)$	$A_{CP}(\rho K)$	ΔC	ΔS
$-0.11 \pm 0.06 \pm 0.03$	$0.18 \pm 0.12 \pm 0.08$	$0.2 \pm 0.13 \pm 0.05$	$0.33 \pm 0.18 \pm 0.03$

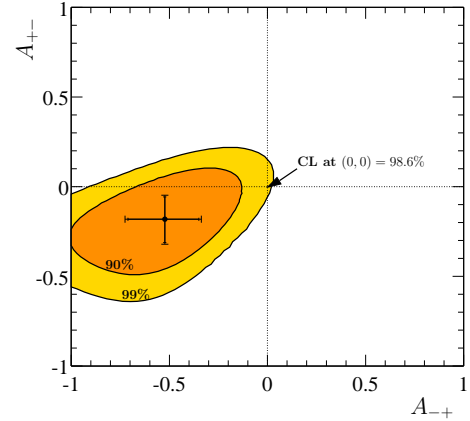
CP-violation, and the quantities $C_{\rho\pi}$ and the charge asymmetry $A_{\rho h} = \frac{N(\rho^+ h^-) - N(\rho^- h^+)}{N(\rho^+ h^-) + N(\rho^- h^+)}$ ($A_{\rho\pi}$ and $A_{\rho K}$) are measures of direct CP-violation. The parameters $\Delta C_{\rho\pi}$ and $\Delta S_{\rho\pi}$ are CP conserving quantities and are labeled as dilution factors. The projection plots in Δt and the corresponding time-dependent asymmetry plot are shown in Fig. 16. The results, including the charge asymmetry for the decay $B \rightarrow \rho K$, are summarized in Table 3.

Figure 16. Time-evolution and asymmetry plot for $B \rightarrow \rho^\pm \pi^\mp$ candidates in the BaBar data.

There is no significant evidence for CP-violation in this mode, but the values of the direct CPV quantities, $C_{\rho\pi}$ and $A_{CP}(\rho\pi)$, both showing about 2σ deviations from zero, deserve a little more attention. In order to present a statistical statement on direct CPV effects in this channel, these quantities are recast in more familiar forms:

$$A_{+-} = \frac{N(\bar{B}^0 \rightarrow \rho^+ \pi^-) - N(B^0 \rho^- \pi^+)}{N(\bar{B}^0 \rightarrow \rho^+ \pi^-) + N(B^0 \rho^- \pi^+)}$$

$$= \frac{A_{CP}^{\rho\pi} - C - A_{CP}^{\rho\pi} \cdot \Delta C}{1 - \Delta C - A_{CP}^{\rho\pi} \cdot C},$$

Figure 17. Confidence intervals for the direct CP-asymmetries A_{+-} and A_{-+} using total error bars (statistical and systematic errors in quadrature).

$$A_{-+} = \frac{N(\bar{B}^0 \rightarrow \rho^- \pi^+) - N(B^0 \rho^+ \pi^-)}{N(\bar{B}^0 \rightarrow \rho^- \pi^+) + N(B^0 \rho^+ \pi^-)}$$

$$= \frac{A_{CP}^{\rho\pi} + C + A_{CP}^{\rho\pi} \cdot \Delta C}{1 + \Delta C + A_{CP}^{\rho\pi} \cdot C}.$$

and plotted in Fig. 17 along with the corresponding confidence level plots. This puts the data point at about 2.5σ away from the origin (zero CPV point).

5.2. Comments on the Decay $B \rightarrow \rho\rho$

Both BaBar and Belle have performed extensive studies of the $B \rightarrow VV$ decays, where V stands for a vector meson (reviewed in the talk by J. Fry at this conference). An important channel among this class of final states, presenting interesting opportunities for measuring α , is the family of $B \rightarrow \rho\rho$ decays, which includes $B^0 \rightarrow \rho^+ \rho^-$, $B^+ \rightarrow \rho^+ \rho^0$ and $B^0 \rightarrow \rho^0 \rho^0$. The $\rho\rho$ system is essentially an analog of the $\pi\pi$ system (with one caveat discussed below), providing a measurement of $\alpha_{eff}^{\rho\rho}$. The decay amplitudes are connected via isospin symmetry and a Quinn-Grossman (type) bound on $|\alpha_{eff}^{\rho\rho} - \alpha|$ can be extracted from information on the mean branching

ratios of the decays $B^0 \rightarrow \rho^0 \rho^0$ and $B^+ \rightarrow \rho^+ \rho^0$. The main difference from the $\pi\pi$ system is in the CP composition of the final state, which in this case can be a mix of CP-odd and CP-even states. In general, the pair of ρ mesons can be in a state of relative orbital angular momentum $L=0$ (S-wave), 1 (P-wave) and 2 (D-wave), thus allowing for both a CP-odd state (transversely polarized ρ) and a CP-even state (longitudinally polarized ρ). The angular analysis of the decays $B^+ \rightarrow \rho^+ \rho^0$ (Belle and BaBar) and $B^+ \rightarrow \rho^+ \rho^-$ (BaBar) have shown that the decays are dominated by the longitudinal polarization (CP-even component) (f_L) .²⁶⁻²⁷ This significantly simplifies the time-dependent measurements which are currently underway, with results expected in the near future. Furthermore, applying the Quinn-Grossman relation to the constraints on branching ratios gives:

$$\sin^2(\alpha_{eff}^{\rho\rho} - \alpha) \leq \frac{(f_L(\rho^0 \rho^0) \times B(\rho^0 \rho^0))}{(f_L(\rho^+ \rho^0) \times B(\rho^+ \rho^0))}$$

resulting in: $|\alpha_{eff}^{\rho\rho} - \alpha| < 19^\circ$, at 90% CL which is already more restrictive on penguin effects than in the $\pi\pi$ system.

6. Reaching γ via the $B \rightarrow DK$ Channel: Interference of $b \rightarrow u(W^- \rightarrow \bar{c}s)$ and $b \rightarrow c(W^- \rightarrow \bar{u}s)$

The family of $B \rightarrow DK$ decays represents a ‘‘penguin free’’ channel for reaching the angle γ . The responsible diagrams are illustrated in Fig. 18. For details of the methods and formulation of strategies for these measurements see the References.²⁹ The amplitude relations below show the connection to the angle γ , which enters via V_{ub} :

$$\begin{aligned} A(B^- \rightarrow \bar{D}^0 K^-) &= |A_1| e^{i\delta_1} e^{i\gamma} \\ A(B^- \rightarrow D^0 K^-) &= |A_2| e^{i\delta_2}, \end{aligned}$$

$$\begin{aligned} A(B^+ \rightarrow D^0 K^+) &= |A_1| e^{i\delta_1} e^{-i\gamma} \\ A(B^+ \rightarrow \bar{D}^0 K^+) &= |A_2| e^{i\delta_2}, \end{aligned}$$

where δ_1 and δ_2 are the CP conserving strong phases. For final states where the D meson decays into a CP-eigenstate (such as $\pi^+ \pi^-$ or ϕK_s^0), D_{cp} , both diagrams contribute, with the corresponding decay amplitudes:

$$A(B^- \rightarrow D_{cp} K^-) = |A_1| e^{i\delta_1} e^{i\gamma} + |A_2| e^{i\delta_2},$$

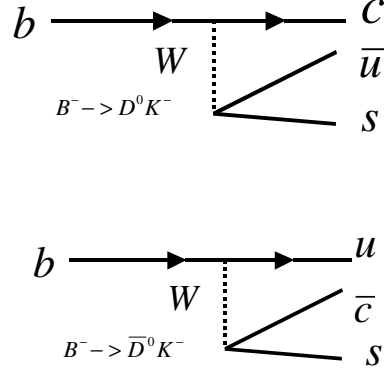


Figure 18. Diagrams of contributions to the decay $B \rightarrow D_{cp} K$. See the text for details.

$$A(B^+ \rightarrow D_{cp} K^+) = |A_1| e^{i\delta_1} e^{-i\gamma} + |A_2| e^{i\delta_2}.$$

The resulting interference effects preserve the sensitivity to the angle γ in the rates and CPV observables. From the experimental point of view, however, the task is difficult: the expected asymmetries are small (the scale set by the relative sizes of the interfering CKM suppressed and favored diagrams) and the D^0 decays into CP-eigenstates are rare. The original proposal by Wyler *et al.*,²⁹ involved construction of the two amplitude triangles in the complex plane using the decay rates, and determination of the angle γ from their mismatch. However, it turns out that in practice when hadronic final states are employed for identifying D meson decays, the $b \rightarrow u$ channel ($B^+ \rightarrow D^0 K^+$) is indistinguishable from the final state $B^+ \rightarrow \bar{D}^0 K^+$ ($b \rightarrow c$) followed by the Double Cabibbo Suppressed Decay of \bar{D}^0 . The alternative set of observables, which have been explored in these channels, consists of the rate ratio and the CP-asymmetry defined as :

$$\begin{aligned} R_{cp} &= \frac{B(B^- \rightarrow D_{cp}^0 K^-) + B(B^+ \rightarrow \bar{D}_{cp}^0 K^+)}{B(B^- \rightarrow D^0 K^-) + B(B^+ \rightarrow \bar{D}^0 K^+)} \\ &= 1 + r_{DK}^2 \pm 2r_{DK} \cos \delta_{DK} \cos \gamma, \end{aligned}$$

$$\begin{aligned} A_{cp} &= \frac{B(B^- \rightarrow D_{cp}^0 K^-) - B(B^+ \rightarrow \bar{D}_{cp}^0 K^+)}{B(B^- \rightarrow D^0 K^-) + B(B^+ \rightarrow \bar{D}^0 K^+)} \\ &= \frac{\pm 2R_{DK} \sin \delta_{DK} \sin \gamma}{1 + r_{DK}^2 \pm 2r_{DK} \cos \delta_{DK} \cos \gamma}, \end{aligned}$$

where the unknown parameters are the ratio of the amplitudes of the $b \rightarrow u$ and the $b \rightarrow c$ transitions (for each decay process), r_{DK} , their relative strong phase δ_{DK} and the angle γ . In principle, all three unknowns can be extracted from the data,

Table 4. Measured Branching ratios for $B \rightarrow DK$ decays

Mode	CLEO	Belle	BaBar
$B^- \rightarrow D^0 K^-$	$(9.9 \pm 1.3 \pm 0.7)\%$	$(7.7 \pm 0.9 \pm 0.6)\%$	$(8.31 \pm 0.35 \pm 0.2)\%$
$B^- \rightarrow D^0 K^{*-}$	$(6.1 \pm 1.6 \pm 1.7) \times 10^{-4}$	$(5.2 \pm 0.5 \pm 0.6) \times 10^{-4}$	$(6.3 \pm 0.7 \pm 0.4) \times 10^{-4}$
$B^- \rightarrow D^{*0} K^{*-}$	$(7.7 \pm 2.2 \pm 2.6) \times 10^{-4}$		$(8.3 \pm 1.1 \pm 1.0) \times 10^{-4}$
$B^0 \rightarrow \bar{D}^0 K^{*0}$		$(4.8 \pm 1.1 \pm 0.5) \times 10^{-5}$	$(3.0 \pm 1.3 \pm 0.6) \times 10^{-5}$
$B^0 \rightarrow \bar{D}^0 K^0$		$(5.0 \pm 1.3 \pm 0.6) \times 10^{-5}$	$(3.4 \pm 1.3 \pm 0.6) \times 10^{-5}$
$B^0 \rightarrow \bar{D}^{*0} K^0$		$< 6.6 \times 10^{-5} (90\% CL)$	
$B^0 \rightarrow \bar{D}^{*0} K^{*0}$		$< 6.9 \times 10^{-5} (90\% CL)$	
$B^0 \rightarrow D^{*0} K^0$		$< 1.8 \times 10^{-5} (90\% CL)$	
$B^0 \rightarrow D^{*0} K^{*0}$		$< 4.0 \times 10^{-5} (90\% CL)$	

Table 5. Measured CP observables for the $B \rightarrow DK$ decays

$B^- \rightarrow D^0 K^-$	$R_1(CP = +1)$	$A_1(CP = +1)$	$R_2(CP = -1)$	$A_2(CP = -1)$
Belle	$1.21 \pm 0.25 \pm 0.14$	$0.06 \pm 0.19 \pm 0.04$	$1.41 \pm 0.27 \pm 0.15$	$-0.19 \pm 0.17 \pm 0.05$
BaBar	$1.06 \pm 0.26 \pm 0.17$	$0.17 \pm 0.23 \pm 0.08$		
$B^- \rightarrow D^0 K^{*-}$				
Belle		$-0.06 \pm 0.33 \pm 0.07$		$0.19 \pm 0.50 \pm 0.04$

when sufficient precision in the measurements has been achieved. The method has also been extended to B^0 decays.

The experiments have covered many of the possible channels in the $B \rightarrow DK$ system,^{30–33} as compiled in Table 4 and Table 5, with several incomplete areas waiting for more data. The Belle collaboration has performed an analysis of the decay $B \rightarrow D^0 K$, using the 3-body decays of D^0 ,³⁴ reporting a 90% CL interval of $61^\circ < \gamma < 142^\circ$.

7. Reaching $2\beta + \gamma$ Through the Decay

$B \rightarrow D^{(*)+} \pi^-$: Interference of the $b \rightarrow c$ and $b \rightarrow u$ Diagram via $B^0 \rightarrow \bar{B}^0$ Mixing

A small interference effect present in the decay $B \rightarrow D^{(*)+} \pi$ provides sensitivity to the phase $2\beta + \gamma$.³⁵ The dominant contributing diagram to this channel is the CKM favored $b \rightarrow c(\bar{u}d)$ transition. A small

contribution is also expected from the diagram involving $B^0 \leftrightarrow \bar{B}^0$ oscillation, followed by the CKM suppressed $\bar{b} \rightarrow \bar{u}(c\bar{d})$ transition. The interference of the two diagrams generates sensitivity to the phase $2\beta + \gamma$, where the mixing diagram contributes to the phase 2β .

As expected the resulting CP-asymmetry is very small, the scale set by the ratio of the amplitudes: $r_{D\pi} = \frac{A(\bar{B}^0 \rightarrow D^- \pi^+)}{A(B^0 \rightarrow D^- \pi^+)} \simeq 0.02$. The experimental analysis involves a time-dependent CP analysis of tagged neutral B decays into this final state. The time evolution relations are:

$$P(B^0 \rightarrow D^\mp \pi^\pm, \Delta t) = Ne^{-\Gamma|\Delta t|} [1 \pm C_{D\pi} \cos(\Delta m_d \Delta t) + S_{D\pi}^\mp \sin(\Delta m_d \Delta t)],$$

$$P(\bar{B}^0 \rightarrow D^\mp \pi^\pm, \Delta t) = Ne^{-\Gamma|\Delta t|} [1 \mp C_{D\pi} \cos(\Delta m_d \Delta t) - S_{D\pi}^\mp \sin(\Delta m_d \Delta t)],$$

where the CP observables are $C_{D\pi} = \frac{1-r_{D\pi}^2}{1+r_{D\pi}^2} \simeq 1$ and

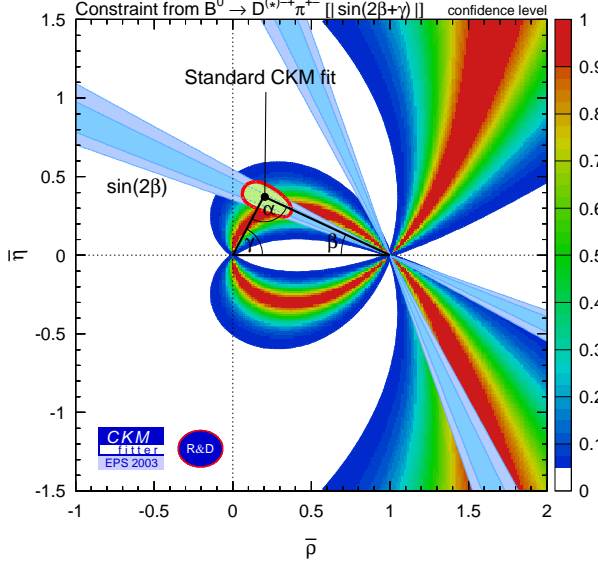


Figure 19. The CKM fit with the constraints from $2\beta + \gamma$ included. (From CKMfitter group (<http://ckmfitter.in2p3.fr/>.)

$S_{D\pi} = \frac{2r_{D\pi}}{1+r_{D\pi}} \sin(2\beta + \gamma \pm \delta_{D\pi})$. Besides $2\beta + \gamma$, the other unknowns in this analysis are $r_{D\pi}$ and the relative strong phase $\delta_{D\pi}$. BaBar and Belle presented preliminary results on time-dependent CP-asymmetries in $B \rightarrow D^{*+}\pi^-$ and $B \rightarrow D^+\pi^-$ at this conference. A summary of the measurements is given below.

BaBar with fully reconstructed decays³⁶

$$\begin{aligned} 2r_{D^*\pi} \sin(2\beta + \gamma) \cos\delta_{D^*\pi} &= -0.068 \pm 0.038 \pm 0.021 \\ 2r_{D^*\pi} \cos(2\beta + \gamma) \sin\delta_{D^*\pi} &= -0.031 \pm 0.070 \pm 0.035 \\ 2r_{D\pi} \sin(2\beta + \gamma) \cos\delta_{D\pi} &= -0.022 \pm 0.038 \pm 0.021 \\ 2r_{D\pi} \cos(2\beta + \gamma) \sin\delta_{D\pi} &= -0.025 \pm 0.068 \pm 0.035. \end{aligned}$$

Belle with fully reconstructed decays³⁷

$$\begin{aligned} 2r_{D^*\pi} \sin(2\beta + \gamma + \delta_{D^*\pi}) &= +0.092 \pm 0.059 \pm 0.016 \pm 0.036(D^*\ell\nu) \\ 2r_{D^*\pi} \sin(2\beta + \gamma - \delta_{D^*\pi}) &= +0.033 \pm 0.056 \pm 0.016 \pm 0.036(D^*\ell\nu) \\ 2r_{D\pi} \sin(2\beta + \gamma + \delta_{D\pi}) &= +0.094 \pm 0.059 \pm 0.013 \pm 0.036(D^*\ell\nu) \\ 2r_{D\pi} \sin(2\beta + \gamma - \delta_{D\pi}) &= +0.022 \pm 0.056 \pm 0.013 \pm 0.036(D^*\ell\nu). \end{aligned}$$

BaBar with partially reconstructed decays³⁶

$$2r_{D^*\pi} \sin(2\beta + \gamma) \cos\delta_{D^*\pi} = -0.064 \pm 0.025 \pm 0.017.$$

The BaBar collaboration has presented limits on $\sin(2\beta + \gamma)$ using an estimate of $r_{D\pi}$ by employing factorization relations and information from the decay $B \rightarrow D_s\pi$, corrected for flavor SU(3) breaking. They perform a χ^2 fit, taking into account estimates of the theoretical and experimental uncertainties to calculate confidence levels as a function of the CPV phase. They set an upper bound of $|\sin(2\beta + \gamma)| > 0.76$ at 90% CL Figure 19 shows the implication of the confidence level information on $\sin(2\beta + \gamma)$ in the (η, ρ) plane, along with the standard “CKM fit”, indicating that the $\sin(2\beta + \gamma)$ information also favors the Standard Model (η, ρ) region.

8. Summary and Conclusion

After establishing that CP-symmetry is broken in B meson decays, the B -factory experiments have been hard at work to examine the consistency of the measurements with the Standard Model predictions and search for new physics effects via possible deviations from the SM. A major focus of the experiments has been on the determination of the CKM unitarity angles $\alpha(\phi_2)$ and $\gamma(\phi_3)$, through a variety of channels and the use of theoretical relations to interpret the results. The BaBar and Belle collaborations have performed measurements of the time-dependent CP observables in the channel $B \rightarrow \pi^+\pi^-$. The results from the two experiments, which are about 2σ apart, do not yet establish CPV in this channel, but are consistent with the expected values from the SM. Significant progress has also been made in identifying and measuring the components of the 2-body charmless B decays, which together with theoretical models and symmetry relations will eventually lead to the determination of the angles α and γ . The BaBar collaboration announced the observation of the decay $B \rightarrow \pi^0\pi^0$, supported by strong evidence from the Belle experiment. New results were also presented on the $B \rightarrow \rho\pi$ decays, including measurements of time-dependent CPV observables in the quasi 2-body channel $B \rightarrow \rho\pi$ by the BaBar collaboration, with hints (at 2σ level) of possible direct CPV effects. Both experiments expect results with amplitude analyses in this channel in the near future. Measurements of the rates and polarization in the $B \rightarrow \rho\rho$ system by Belle and BaBar indicate that this is a potentially powerful channel for the

determination of α . The experiments have also presented results, albeit with large errors, on branching ratios and CPV observables in the $B \rightarrow DK$ system, which is sensitive to the angle γ , and time-dependent CPV analyses of $B \rightarrow D^{*+}\pi^-$ with information on $\sin(2\beta + \gamma)$. At the current level of experimental and theoretical accuracies, all of the measurements in this area can be accommodated in the SM and the information on α and γ are consistent with the CKM picture. However, this is just the beginning of the experimental investigation of these channels for CPV information. With the expected significant increase in the data from the B -factories in the next few years, the goal is to extract information on α and γ through as many channels as possible, thus reduce both the experimental and theoretical uncertainties on these quantities.

Acknowledgments

I wish to thank my colleagues on the BaBar and Belle experiments who are responsible for most of the experimental results presented here. I am also grateful to M. Gronau, J. L. Rosner, A. Hoecker, H. Lacker, T. Browder, J. Smith, J. Alexander, P. Chang, B. Cahn, J. Olsen, A. Farbin, E. Rosenberg, D. Roberts and J. Fry for their comments and help in the preparation of the talk and this document. I wish to thank the organizers of the 2003 Lepton-Photon Symposium for their support. This work was partially supported by a grant from the United States Department of Energy.

References

1. M. Kobayashi and T. Maskawa, *Prog. Th. Phys.* **49**, 652 (1973).
2. L. Wolfenstein, *Phys. Rev. Lett.* **51**, 1945 (1983).
3. A. Hoecker, H. Lacker, S. Laplace and F. Le Diberder, *Eur. Phys. Jour. C* **21**, 225 (2001) (hep-ph/0104062).
4. BaBar Collaboration, B. Aubert *et al.*, *Phys. Rev. Lett.* **89**, 201802 (2002); Belle Collaboration, K. Abe *et al.*, *Phys. Rev. D* **66**, 071102 (2002).
5. Heavy Flavor Averaging Group (see the webpage <http://www.slac.stanford.edu/xorg/hfag/>).
6. M. Beneke, G. Buchalla, M. Neubert and C. T. Sachrajda, *Phys. Rev. Lett.* **83**, 1914 (1999).
7. Y. Keum, H. Li and A. I. Sanda, *Phys. Lett. B* **504**, 6 (2001).
8. B. Aubert *et al.* (BaBar Collaboration), *Phys. Rev. Lett.* **89**, 281802 (2002).
9. K. Abe *et al.* (Belle Collaboration), *Phys. Rev. D* **68**, 012001 (2003).
10. B. Aubert *et al.* (BaBar Collaboration), hep-ex/0308012.
11. S.H. Lee and K. Suzuki *et al.* (Belle Collaboration), hep-ex-0308040.
12. M. Gronau and D. London, *Phys. Rev. Lett.* **65**, 3381 (1990).
13. H. R. Quinn and A.E. Snyder, *Phys. Rev. D* **48**, 2139 (1993).
14. M. Gronau and J.L.Rosner, *Phys. Rev. D* **65**, 093012 (2002).
15. M. Gronau and J.L.Rosner, *Phys. Rev. D* **65**, 013004 (2001).
16. J.L. Rosner, hep-ph/0305315; M. Gronau, hep-ph/0306308.
17. R. Fleischer, hep-ph/0306270.
18. A. Hoecker, H. Lacker, M. Pivak and L. Roos, LAL 02-103.
19. Y. Grossman and H.R. Quinn, *Phys. Rev. D* **58** 017504 (1998).
20. J. Charles, *Phys. Rev. D* **59** 054007 (1999).
21. M. Gronau, D. London, N. Sinha and R. Sinha, *Phys. Lett. B* **514**, 315 (2000).
22. M. Gronau, J.L. Rosner and D. London, *Phys. Rev. Lett.* **73**, 21 (1994); O. F. Fernandez *et al.*, *Phys. Lett. B* **333**, 500 (1994); R. Fleischer, *Int. Jour. Mod. Phys. A* **12**, 2459 (1997).
23. F. Fleischer and T. Mannel, *Phys. Rev. D* **57**, 2752 (1998).
24. M. Gronau D. London and J.L.Rosner, *Phys. Rev. Lett.* **73**, 21 (1994).
25. B. Aubert *et al.* (BaBar Collaboration), hep-ex/0307087 and hep-ex/0306063.
26. J.Zhang, M.Nakao *et al.* (Belle Collaboration), hep-ex/0306007.
27. B. Aubert *et al.* (BaBar Collaboration), hep-ex/0308026.
28. B. Aubert *et al.* (BaBar Collaboration), hep-ex/0308024.
29. M. Gronau and D. Wyler, *Phys. Lett. B* **265**, 172 (1991); D. Atwood, I. Dunietz and A. Soni, *Phys. Rev. Lett.* **78**, 3257 (1997).
30. S.K.Swain, T.E.Browder *et al.* (Belle Collaboration), *Phys. Rev. D* **68**, 051101 (2003).
31. P.Krokovny *et al.* (Belle Collaboration), *Phys. Rev. Lett.* **90**, 141802 (2003).
32. K. Abe *et al.* (Belle Collaboration), hep-ex/0307074.
33. B. Aubert *et al.* (BaBar Collaboration), hep-ex/0207087 and hep-ex/0307036.
34. K. Abe *et al.* (Belle Collaboration), hep-ex/0308043.
35. R. G. Sachs, Enrico Fermi Institute Report, EFI-85-22 (1985) (unpublished); I. Dunietz and R.G. Sachs, *Phys. Rev. D.* **37**, 3186 (1988); *Phys. Lett. B* **427**, 179 (1998).
36. B. Aubert *et al.* (BaBar Collaboration), hep-ex/0308018 and hep-ex/0307036.
37. K. Abe *et al.* (Belle Collaboration), hep-ex/0308048.

DISCUSSION

Tom Browder (Univ. of Hawaii): This is related to the issue about final-state interactions in $B \rightarrow \rho\pi$. Belle has presented evidence for $B \rightarrow \rho^0\pi^0$, which is perhaps a hint that there are large final-state phases in that system as well?

Abolhassan Jawahery: That's a good comment. Maybe the theorists want to comment on it. I will leave it at that.

Ikaros Bigi (Univ. of Notre Dame): You talked about the new BaBar result on $B \rightarrow \pi\pi$, one of my interests is to show deviations from the Superweak scenario with the new BaBar result. How far away from pure Superweak CP-violation are you?

Abolhassan Jawahery: You mean with pure Superweak we have $S = \sin(2\beta)$, so is $S = \sin(2\beta)$? We cannot say it is not. I think with the numbers we have, we are within 1σ of that.

Klaus Schubert (TU Dresden): This is a comment to Bigi's question. As long as $\cos(2\beta)$ and $\cos(2\alpha_{eff})$ are not measured, direct CP-violation in $\lambda_{(ccK)}/\lambda_{(\pi\pi)}$ can not be established with the present data on $\sin(2\beta)$ and $\sin(2\alpha_{eff})$.

Ikaros Bigi (Univ. of Notre Dame): We can discuss this on Thursday, in the breakout session.